ACS Medicinal Chemistry Letters

Letter

Design of KDM4 Inhibitors with Anti-Proliferative Effects in Cancer Models

Young K. Chen, Tiziana Bonaldi, Alessandro Cuomo, Joselyn R. Del Rosario, David J. Hosfield, Toufike Kanouni, Shih-chu Kao, Chon Lai, Neethan A. Lobo, Jennifer Matuszkiewicz, Andrew McGeehan, Shawn M. O'Connell, Lihong Shi, Jeffrey A. Stafford, Ryan K. Stansfield, James M. Veal, Michael S. Weiss, Natalie Y. Yuen, and Michael B Wallace

ACS Med. Chem. Lett., **Just Accepted Manuscript** • DOI: 10.1021/acsmedchemlett.7b00220 • Publication Date (Web): 27 Jul 2017

ACS Publications

ACS Medicinal Chemistry Letters is published by the American Chemical Society. 1155 Sixteenth Street N.W., Washington, DC 20036

Design of KDM4 Inhibitors with Anti-Proliferative Effects in Cancer Models

Young K. Chen,[†] Tiziana Bonaldi,[#] Alessandro Cuomo,[#] Joselyn R. Del Rosario,[†] David J. Hosfield,[ϕ] Toufike Kanouni,[†] Shih-chu Kao,[‡●] Chon Lai,[†] Neethan A. Lobo,[‡] Jennifer Matuszkiewicz,[†] Andrew McGeehan,[‡] Shawn M. O'Connell,[†▲] Lihong Shi,[†] Jeffrey A. Stafford,[†■] Ryan K. Stansfield,[†■] James M. Veal,[†■] Michael S. Weiss,[‡□] Natalie Y. Yuen,[‡] and Michael B. Wallace[†*]

[†]Celgene Quanticel Research, 10300 Campus Point Drive, Suite 100, San Diego, CA, 92121

[‡]Celgene Quanticel Research, 1500 Owens Street, Suite 500, San Francisco, CA, 94158

[#]Department of Experimental Oncology, European Institute of Oncology, Via Adamello 16, 20139 Milano, Italy

[ϕ] Ben May Department for Cancer Research, University of Chicago, 929 E. 57th St., Chicago, IL, 60637

KEYWORDS: Epigenetics, histone demethylase, KDM4, JMJD2, synthesis, cancer.

ABSTRACT: Histone lysine demethylases (KDMs) play a vital role in the regulation of chromatin-related processes. Herein we describe our discovery of a series of potent KDM4 inhibitors that are both cell permeable and anti-proliferative in cancer models. The modulation of histone H3K9me3 and H3K36me3 upon compound treatment was verified by homogeneous time-resolved fluorescence assay and by mass spectroscopy detection. Optimization of the series using structure-based drug design led to compound **6** (QC6352), a potent KDM4 family inhibitor that is efficacious in breast and colon cancer PDX models.

The epigenetic alteration of histones by reversible methylation of histone lysine residues constitutes a key mechanism of gene activation and silencing. The complementary activities of lysine methyl transferases (KMTs) and lysine demethylases (KDMs) maintain homeostasis in healthy cells. However, dysregulation and overexpression of KMTs or KDMs are hallmarks of a number of pathologies, including cancers.[1,2] As a result, these targets have generated interest as therapeutic targets in oncology. While advances have been made in the area of KMT inhibitors and lysine demethylase 1 (LSD1, or KDM1a) inhibitors,[3,4] few inhibitors of the Jumonji family of histone demethylases have been reported that show potent cellular anti-proliferative effects.[5] Currently there are no known clinical trials for inhibitors of Jumonji KDMs.

The Jumonji KDM4 family are site-specific *N*-methyl lysine demethylases which function enzymatically by way of an iron and 2-oxoglutarate (2-OG) dependent oxygenase mechanism. The KDM4 family members catalyze the demethylation of histone-3-lysine-9 trimethyl and dimethyl (H3K9me3/H3K9me2), which is a process linked to transcriptional activation.[6-8] Additionally, KDM4A-C catalyze the demethylation of histone-3-lysine-36 trimethyl and dimethyl (H3K36me3/H3K36me2), which is associated with gene repression, aberrant initiation, and the prevention of transcriptional elongation.[7-9] KDM4 family members have been implicated in events that may contribute to cancer development, such as cell-cycle progression,[10,11] hypoxia,[11-13] and transient site-specific copy gain.[14]

KDM4C has been implicated as a driver gene within the 9p23-24 amplicon, which is amplified in multiple tumor types, including esophageal and breast cancers.[15] KDM4A is associated with specific copy number gain of 1q12-q21, a region linked to chemotherapy resistance in ovarian cancer and multiple myeloma.[12,14] KDM4 genes and proteins are overexpressed in numerous tumor types including breast, colorectal, pancreatic, lymphoma, and gastric cancers.[16-19] KDM4 family members also play an important role in the epigenetic regulation of embryonic stem cell identity.[20-21]

Due to its highly polar 2-OG binding pocket, the Jumonji histone demethylase class of protein presents considerable challenges for small-molecule drug discovery. Several inhibitor leads have been reported which contain a carboxylic acid functionality, but they have little or no cellular activity.[22-24] To address this liability, strategies involving bioisosteres in place of carboxylic acids have been utilized.[25] Pro-drug approaches, which can add complexity to the drug development process, have also been employed.[26] Despite the inherent challenges, drugs containing carboxylic acids are among the most successfully marketed drugs.[27] Furthermore, carboxylic acid 2-OG binding site inhibitors are currently being advanced for prolyl-hydroxylase domain containing protein 2 (PHD2).[28] We felt that developable carboxylic acid inhibitors could be discovered for the KDM4 family as well, as long as certain physiochemical property principles were taken into account. A measured approach balancing the polarity of the carboxylic acid functionality with lipophilicity and judicious placement of a limited number of heteroatoms could yield inhibitors with good drug-likeness.[25] Herein, we report our discovery of cell permeable, selective KDM4 small molecule inhibitors that

demonstrates potent on-target anti-proliferative effects in cancer cell models.

Our efforts towards discovery of a KDM4 inhibitor began with a screen of a subset of fragments related to pyridine-2,4-dicarboxylic acid, a well-known 2-OG mimetic and pan KDM inhibitor (KDM4C IC_{50} = 19 nM) that has been co-crystallized in KDM4A.[29] Although less potent than 2,4-PDCA at inhibiting KDM4C enzymatic activity, we considered the fragment lead 3-(methylamino)isonicotinic acid **1** to be a more attractive starting point for lead optimization. Compound **1** exhibits promising enzymatic potency (KDM4C IC_{50} = 1400 nM) while containing just a single coordinative interaction to the Fe(II) cofactor rather than the bidentate chelator functionality of 2,4-PDCA. In addition, the 3-amino functionality provides an internal hydrogen bond with the 4-position carboxylate that could impart improved physical properties (Chart 1). Finally, **1** also provides a handle for further substitution at a favorable vector for SAR exploration, based on the expected binding mode. 3-Aminoisonicotinic acid inhibitors have been reported, with some compounds demonstrating modest cellular effects (GSK, Chart 1).[30]

Chart 1. 2,4-Pyridine Carboxylic Acid, Compound 1, and GSK Inhibitor

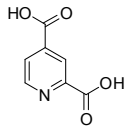

2,4-PDCA
KDM4C IC_{50} = 19 nM

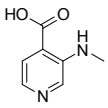

1
IC_{50} = 1400 nM

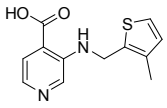

GSK Inhibitor

From exploration of substitutions off of the 3-aminoisonicotinic acid nitrogen, we identified the tetrahydronaphthalene compound **2** (Chart 2) as a potent inhibitor of KDM4C (IC_{50} = 12 nM). KDM4C was originally cloned from the esophageal cell line KYSE-150,[28] and shRNA knockdown of KDM4C in KYSE-150 has been shown to impair cell proliferation.[6] Therefore, we chose to utilize the same KYSE-150 line for a cell-based anti-proliferation assay measuring incorporation of BrdU. Tested as its racemate, compound **2** demonstrated measurable inhibition of cell proliferation (EC_{50} = 6 μM) in the KYSE-150 cell line. Given this result, the enantiopure compounds **2a** and **2b** were prepared. The *R*-enantiomer **2a** was determined to be the active enantiomer (KDM4C IC_{50} = 8 nM, KYSE-150 cell EC_{50} = 4 μM), while the *S*-enantiomer **2b** was shown to be relatively inactive (KDM4C IC_{50} > 2 μM, KYSE-150 cell EC_{50} > 100 μM).

Chart 2. Tetrahydronaphthalene Lead 2 and Enantiomers

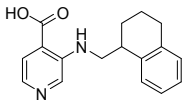

2
KDM4C IC_{50} = 12 nM
KYSE-150 EC_{50} = 6 μM

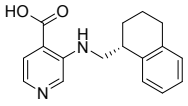

2a
IC_{50} = 8 nM
EC_{50} = 4 μM

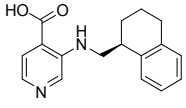

2b
IC_{50} > 2000 nM
EC_{50} > 100 μM

Molecular modelling of compound **2a** suggested that the 6-position of the tetrahydronaphthalene ring would be optimal for further elaboration and SAR development. Substitution with a 6-position methoxy group gave compound **3** (Figure 1a), which retained the enzymatic inhibitory properties in the lead (KDM4C IC_{50} = 6 nM) while improving anti-proliferative effects in the KYSE-150 Cell BrdU assay (EC_{50} = 830 nM). Compound **3** was co-crystallized with KDM4A and refined to 2.5 Å resolution (Figure 1b). Consistent with other reported KDM4 structures,[29,30] the pyridinecarboxylate core binds to the Jumonji C domain and mimics the key 2-OG interactions. The pyridine nitrogen forms a single dative bond with the Ni (Fe surrogate) metal, while the pyridyl ring pi-stacks with F185 and the carboxylic acid forms important hydrogen bond interactions with Y132 and K206. The tetrahydronaphthalene ring system extends into the pocket formed by residues N86, I71, Q73, Y132, A134, D135, and Y177, with the phenyl ring of the tetrahydronaphthalene proximal to K241. The C-C bond angles of the structure refined with both enantiomers are consistent with the assignment of compound **3** as the *R*-enantiomer. The tetrahydronaphthalene 6-position methoxy group is directed towards the backbone of H240, with space available for further substitution.

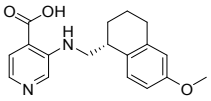

Compound **3**
KDM4C IC_{50} = 6 nM
KYSE-150 EC_{50} = 830 nM

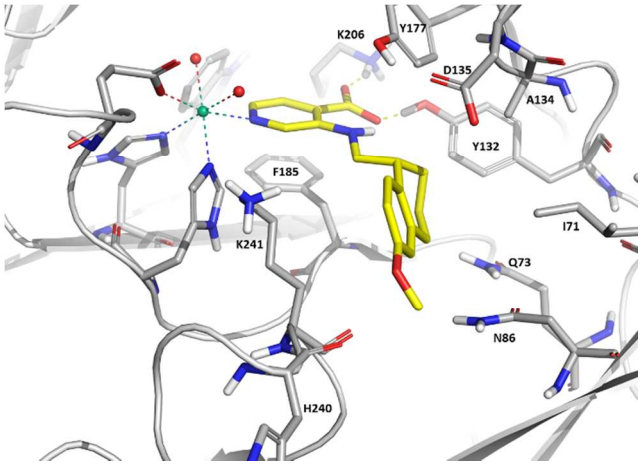

Figure 1. Co-crystal structure of compound **3** in the KDM4A active site. PDB code 5VMP.

In order to assess cellular on-target engagement of the compounds, we examined histone post-translational modification patterns of inhibitor-treated cells by mass spectrometry (MS) analysis. KYSE-150 cells were treated with compound **3** at both 2 μM for 24 hours, and 300 nM for 96 hours. Untreated and treated cells were harvested and histones purified using a standard strong-acidic extraction protocol from fractionated nuclei.[31,32] Purified histone octamers were then subjected to in-gel chemical alkylation with D6-acetic anhydride, followed by trypsin digestion.[33,34] The resulting histone peptide fragments were subjected to high resolution UHPLC-MSMS analysis. Three histone residues of interest—H3K4, H3K9 and H3K36 in their various methylation states (me1/me2/me3)—were examined. MaxQuant software was used to assign peptide sequences and identify modified sites from the MS raw data and relative quantitation of each differentially modified histone peptide was calculated as peptide relative abundance percentage (RA%) using an intensity-based approach (see Supplemental).

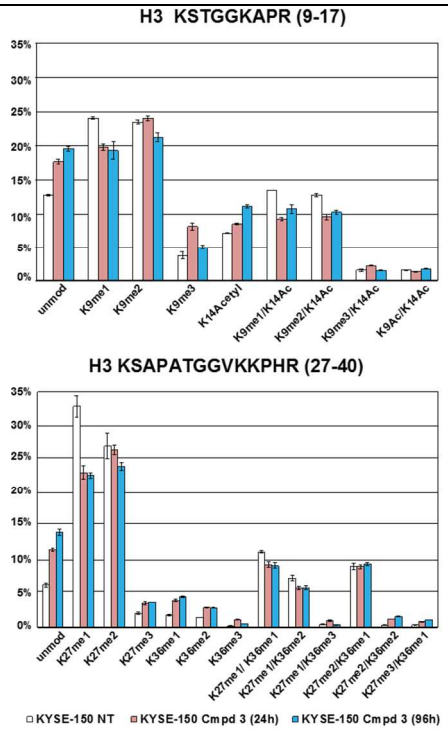

Figure 2. MS intensity-based quantitation of H3 modified peptides (9-17) and (27-40) from KYSE-150 cells treated with compound **3**. Percent Relative Abundances (%RAs) were calculated for all differentially modified forms of peptides (9-17) and (27-40) (top and bottom, respectively). A significant increase ($p<0.01$ two-sample t-test) was detected for both K9me3 and K36me3 at 24 or 96 hours of treatment, relative to the corresponding %RAs of untreated (NT) cells. Error bars represent the standard error of the mean from 5 technical replicates (Supplementary Table 2).

As displayed in Figure 2, the effects of treatment were more pronounced at the 24-hour time point, using the higher inhibitor concentration treatment. At this time point, treated KYSE-150 cells exhibited an increase in both H3K9me3 (>2-fold) and H3K36me3 (>6-fold). Changes in the H3K4me2/me3 methylation states were below the detectable limits (see Supplemental Table 2 for the annotation of RA% for each modified peptide and the corresponding statistical analysis). An in-depth analysis of peptide H3(27-40) revealed that K27me3 is also up-regulated at 24 and 96 hours relative to untreated cells. This finding could be explained either by an indirect, adaptive effect of the cell to compound **3** treatment, or by the recent evidence suggesting that H3K27me3 is a novel KDM4 substrate.[35]

To confirm our MS results, we developed a cell-based MOA assay to measure relevant histone methyl mark changes. KYSE-150 cells were engineered to overexpress KDM4C using a lentiviral transfection (KYSE-150^{+KDM4C}). Consistent with the mechanism of KDM4 demethylase activity, a decrease in H3K9me3 and H3K36me3 levels was observed with the engineered overexpression of KDM4C as compared to the non-transfected KYSE-150 (Supplementary Figure 1). The dynamic range of the changes for H3K36me3 were more pronounced than that for H3K9me3, and thus more amenable to an accurate read-out without baseline interference. Furthermore, we viewed the consistency afforded by the stably transfected cell line to be more fitting for a MOA assay to guide SAR development. The KYSE-150^{+KDM4C} mutant was treated with inhibitor **3** at various test concentrations, and H3K36me3 was measured at 24 hours in a HTRF® assay. A dose-responsive increase in H3K36me3 was clearly demonstrated with an EC_{50} value of 560 nM, a value similar in magnitude with its anti-proliferative effects. In contrast, the negative control compound **2b** demonstrated no observable H3K36me3 induction.

Using the structural information from compound **3**, we designed the derivatives **4**—**6** (Table 1) to impart favorable hydrophobic interactions and improve cellular permeability. In addition, we surveyed heteroatom linkers to determine the optimal vector off of the tetrahydronaphthalene 6-position. We were pleased to discover that compounds **4**—**6** displayed potent KDM4C enzymatic activity, with the H3K36me3 MOA tracking with anti-proliferative effects. Compound **6** (also known as QC6352) showed the most promising cellular potency (KYSE-150 EC_{50} = 3.5 nM, H3K36 MOA = 1.5 nM). The compounds were also inactive in a normal fibroblast cell line (IMR-90), demonstrating that they are not general cytotoxic agents.

Under our enzymatic assay conditions, compounds with high lipophilicity tended to plateau at around 40 nM. This could be attributed in part to the limitations of the enzymatic assay for compounds with high plasma protein binding. In fact, the enzymatic potency of compound **6** (human PPB = 99.9%) improved from 35 nM to 9 nM when the enzymatic assay was run with a lower BSA concentration (0.02 mg/mL instead of 0.2 mg/mL BSA). This apparent right-shift in biochemical activity of lipophilic compounds containing carboxylic acids has been documented.[36] The cell permeability of the compounds could also be a factor impacting their cellular potency, as the permeability measured by PAMPA improved from compound **3** to compounds **5** and **6**. Compound **6** was enzymatically potent across the KDM4 family, and highly selective against other KDM family members, with the exception of KDM5B (Table 2). Although the inhibitor is 7 to 20-fold more potent for KDMs, the KDM5B activity remains significant (IC_{50} = 750 nM). Therefore, we are unable to rule out the possibility of some KDM5 family contribution to the observed phenotype.

Table 1. KDM4C Inhibition, KYSE-150 and IMR-90 Cell Viability, H3K36me3 Mechanism of Action (MOA) Increase, cLogD, and PAMPA Permeability for Compound 3—6.

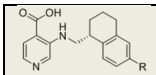	R	KDM4C IC_{50} (nM)	KYSE-150 EC_{50} (nM)	H3K36me3 MOA EC_{50} (nM)	IMR-90 EC_{50} (nM)	cLogD	PAMPA permeability (nm/s)
3	OMe	6 ± 2	830 ± 150	560 ± 200	>30,000	0.27	18.42
4	OPh	17 ± 9	150 ± 10	32 ± 12	>30,000	1.93	32.25
5	SPh	48 ±7	99 ±16	19 ± 5	>30,000	2.61	51.50
6	N(Me)Ph	35 ± 8	3.5 ± 1	1.3 ±0.3	>30,000	2.09	51.18

Table 2. Enzymatic data for compound **6** (QC6352) for KDM4 family isoforms, along with selectivity data for other KDM family members. Data are derived from duplicate data points, and IC_{50} values are reported as the mean of multiple experiments ± s.e.m.

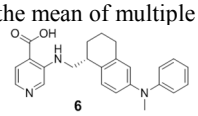

6

KDM	Compound **6** IC_{50} (nM)	KDM	Compound **6** IC_{50} (nM)
KDM2B	>4,000	KDM4C	35 ± 8
KDM3A	>4,000[a]	KDM4D	104 ± 18
KDM3B	>4,000[a]	KDM5B	750 ±170
KDM4A	104 ± 10	KDM6B	>4,000
KDM4B	56 ± 6	PHF8	>4,000[a]

[a]Values derived from biochemical assay without pre-incubation.

The synthesis of the lead compound **6** is described and depicted in Scheme 1. Cyanation of 6-bromochromanone **7** followed by acidic hydrolysis yielded the amide intermediate **8**. Subsequent asymmetric reduction was carried out in the presence of $Ru(OAc)_2$[*S*-binap] to give the *R*-enantiomer **9** in high enantiomeric excess (> 96% ee).[37] Borane reduction of the amide gave the amine **10**. A chemo-selective Buchwald-Hartwig cross-coupling of the amine with methyl 3-bromo-isonicotinate proceeded to give intermediate **11** in moderate yield. A second Buchwald-Hartwig coupling of compound **11** with methyl 3-bromo-isonicotinate followed by saponification gave the final carboxylic acid inhibitor **6**.

Scheme 1. Synthesis of Compound 6

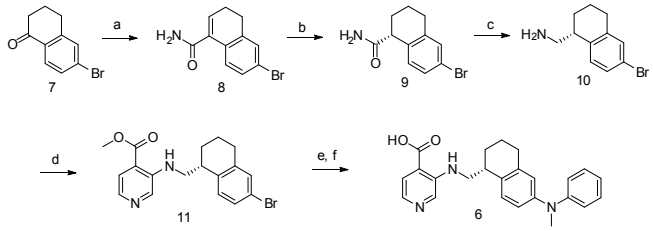

[a]Reagents and conditions: (a) TMSCN, ZnI_2, toluene, 60 ºC; H_2SO_4, AcOH, H_2O, 105 ºC, 80%, (b) H_2, $Ru(OAc)_2$[*S*-binap], THF, MeOH, 77%, > 96% ee, (c) BH_3-THF, THF, 55 ºC, 79%, (d) methyl 3-bromo-isonicotinate, Xantphos, $Pd_2(dba)_3$, Cs_2CO_3, toluene, 120 ºC, 50%, (e) *N*-methyl-aniline, Xantphos, $Pd_2(dba)_3$, Cs_2CO_3, toluene, 128 ºC, 79%, (f) 1N NaOH, MeOH, 89%.

The co-crystal structure of compound **6** bound to KDM4A was solved at a resolution of 2.1 Å (Figure 3). As expected, the inhibitor makes similar interactions to compound **3** in the 2-OG pocket, with the pyridyl nitrogen ligating the active site Ni^{2+} ion while Y132 and K206 form key hydrogen bonds with the carboxylic acid. The methyl group of the *N*-methylaniline substituent packs against N86 and the H240 carbonyl. The edge of the phenyl ring interacts with the R239/H240 loop, and the phenyl group fills the cleft that extends towards the C-terminal region loop containing the residues 309-313. The ligand stereocenter is again unambiguous as the *R*-enantiomer.

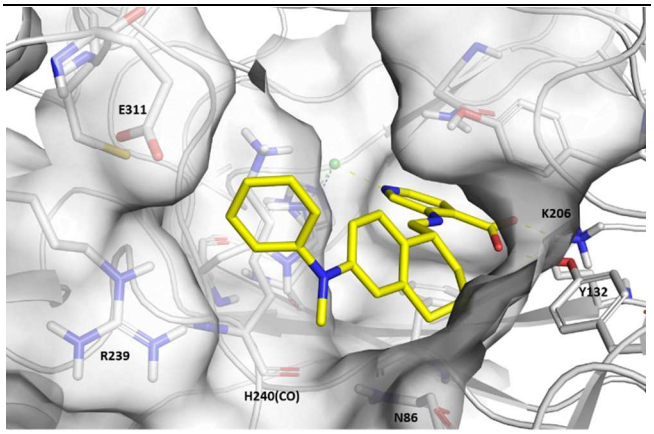

Figure 3. Co-crystal structure of compound **6** (QC6352) in the KDM4A active site. PDB code 5VGI.

With an intent to understand the activity of these KDM4 inhibitors in more pharmacologically relevant models, we tested compound **6** in 3D organotypic cell cultures ("organoids"), which were derived from breast and colon primary patient samples. Both inhibition of colony formation and inhibition of cell viability were determined in BR0869f, a HER2-positive patient-derived breast cancer organoid model, and in SU60, a patient-derived colon cancer organoid model. Compound **6** demonstrated an IC_{50} of 5 nM in BR0869f after a 5-day incubation, and an IC_{50} of 13 nM in the SU60 model.

The pharmacokinetic parameters of compound **6** were determined in female CD-1 mice. After intravenous dose administration (5 mg/kg), compound **6** displayed a low systemic clearance of 6.9 mL/min/kg and a low volume of distribution of 675 mL/kg. Compound **6** was readily absorbed after oral administration (dose = 10 mg/kg) with an AUC of 10,400 ng/mL*hr and an oral bioavailability of 30%.

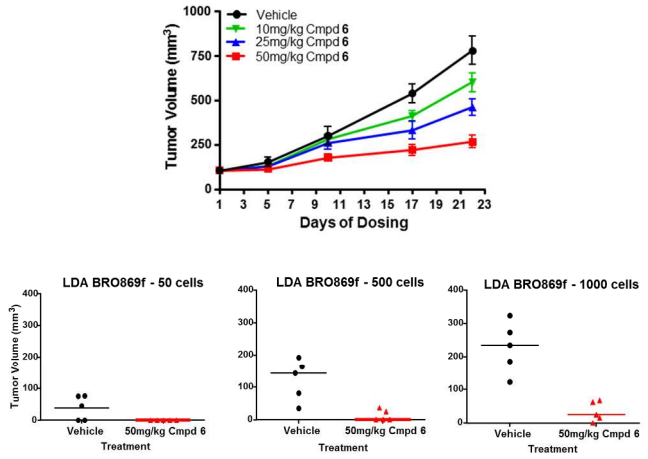

Figure 4. a) Mouse in vivo efficacy of compound **6** in BR0859f xenograft model, dosed BID on a 5 on/2 off schedule. The tumor volumes are reported as the mean of each 8-animal group ± s.e.m. b) Compound **6** shows effects on TIC population in the BR0869f model. Each point represents the tumor volume of a mouse that was inoculated with dissociated cells (50, 500, or 1000 cells) from either the BRO869f xenograft study vehicle group or the 50 mg/kg BID group. The median value is depicted with a line.

Given its potent in vitro effects and suitable PK properties, compound **6** was progressed in vivo utilizing the BR0869f PDX model in mice. The compound was dosed BID on a 5on/2off schedule for 22 days at three dose levels—10 mg/kg, 25 mg/kg, and 50 mg/kg. The rate of tumor growth was diminished in a dose-dependent manner versus the vehicle control (Figure 4a), with tumor growth inhibitions (TGIs) of 22%, 36% and 61%, respectively. The animals' overall body weights remained constant for each group, and the animals appeared in good health (Supplemental Figure 3).

To determine the effects of KDM4 inhibition on tumor initiating cell (TIC) frequency in breast cancer tumors, we evaluated the tumorigenic potential of BR0869f xenograft cells post treatment with compound **6** versus vehicle. At the end of dosing, dissociated cells (50 to 1000) from the 50 mg/kg BID group and the vehicle control group were injected subcutaneously in a limiting dilution manner into NSG mice, and tumor volumes were measured (Figure 4b). The number of cells required for tumor formation was reduced in the compound **6** treated group, and the reduction in TIC frequency was greater than 14-fold.

In summary, we have developed a novel series of potent KDM4 inhibitors with promising selectivity from a small fragment lead using structure-based design. These inhibitors are strongly anti-proliferative in KYSE-150 cells and demonstrate effects on histone methyl marks consistent with inhibiting KDM4 demethylase activity in the same cell line. SAR development led to the potent and efficacious inhibitor compound **6** (QC6352), which has excellent physical properties and drug-like characteristics. Compound **6** showed favorable in vivo efficacy in a breast cancer PDX model and reduced the tumor initiating cell populations which are associated with resistance to chemotherapy treatments.

ASSOCIATED CONTENT

Supporting Information

The Supporting Information is available free of charge on the ACS Publications website.

Experimental details on all compounds and characterizing data, in vitro biological methods, MS methods, and in vivo methods (PDF)

AUTHOR INFORMATION

Corresponding Author

*E-mail: mwallace@celgene.com

Present Addresses

• Benitec Biopharma, 3940 Trust Way, Hayward, CA 94545

▲ Pfizer Inc. Oncology R&D, Epigenetics, 10724 Science Center Drive, San Diego, CA 92121

■ Jecure Therapeutics, Inc., 4757 Nexus Center Drive, Suite 150, San Diego, CA 92121

□ Bristol-Myers Squibb, 700 Bay Rd, Suite A, Redwood City, California, 94063

Author Contributions

Y.K.C., T.K., J.A.S., and M.B.W. led the medicinal chemistry efforts. S.K., C.L., N.A.L., J.M., S.M.O., L.S., and M.S.W. were involved in protein production and biological assay development, execution, and analysis. J.R.D.R., A.M., R.K.S., and N.Y.Y. were responsible for the in vivo studies and analysis. T.B. and A.C. performed the histone MS study. D.J.H. and J.M.V. were involved in the crystallography experiments and analysis.

ACKNOWLEDGMENTS

The authors thank the following scientists for their valuable assistance: Sami Bahmanyar, Robert Cho, Laure Escoubet, Xiaobo Li, Christopher C. Park, and Jianchun Xu. We thank Dongming Qian and Viva Biotech for diffraction data collection. We also thank Dr. Roland Schuele at the University of Freiburg for our continuing collaboration related to QC6352.

REFERENCES

(1) Dimitrova, E.; Turberfield, A. H.; Klose, R. J., Histone demethylases in chromatin biology and beyond. *EMBO Rep.* **2015**, *16* (12), 1620-39.

(2) Rotili, D.; Mai, A., Targeting histone demethylases: a new avenue for the fight against cancer. *Genes Cancer* **2011**, *2* (6), 663-79.

(3) Tian, X.; Zhang, S.; Liu, H. M.; Zhang, Y. B.; Blair, C. A.; Mercola, D.; Sassone-Corsi, P.; Zi, X., Histone lysine-specific methyltransferases and demethylases in carcinogenesis: new targets for cancer therapy and prevention. *Curr. Cancer Drug Targets* **2013**, *13* (5), 558-79.

(4) Mohammad, H. P.; Smitheman, K. N.; Kamat, C. D.; Soong, D.; Federowicz, K. E.; Van Aller, G. S.; Schneck, J. L.; Carson, J. D.; Liu, Y.; Butticello, M.; Bonnette, W. G.; Gorman, S. A.; Degenhardt, Y.; Bai, Y.; McCabe, M. T.; Pappalardi, M. B.; Kasparec, J.; Tian, X.; McNulty, K. C.; Rouse, M.; McDevitt, P.; Ho, T.; Crouthamel, M.; Hart, T. K.; Concha, N. O.; McHugh, C. F.; Miller, W. H.; Dhanak, D.; Tummino, P. J.; Carpenter, C. L.; Johnson, N. W.; Hann, C. L.; Kruger, R. G., A DNA hypomethylation signature predicts antitumor activity of LSD1 inhibitors in SCLC. *Cancer Cell* **2015**, *28* (1), 57-69.

(5) Labelle, M.; Boesen, T.; Khan, Q.; Vakiti, R. R.; Sharma, U.; Yang, Y.; Mehrotra, M.; Saraswat, N.; Ullah, F. Inhibitors of histone demethylases. US 2016/0237037.

(6) Cloos, P. A.; Christensen, J.; Agger, K.; Maiolica, A.; Rappsilber, J.; Antal, T.; Hansen, K. H.; Helin, K., The putative oncogene GASC1 demethylates tri- and dimethylated lysine 9 on histone H3. *Nature* **2006**, *442* (7100), 307-11.

(7) Klose, R. J.; Yamane, K.; Bae, Y.; Zhang, D.; Erdjument-Bromage, H.; Tempst, P.; Wong, J.; Zhang, Y., The transcriptional repressor JHDM3A demethylates trimethyl histone H3 lysine9 and lysine36. *Nature* **2006**, *442* (7100), 312-316.

(8) Kouzarides, T., Chromatin modifications and their function. *Cell* **2007**, *128* (4), 693-705.

(9) Wagner, E. J.; Carpenter, P. B., Understanding the language of Lys36 methylation at histone H3. *Nat. Rev. Mol. Cell Biol.* **2012**, *13,* 115-126.

(10) Kupershmit, I.; Khoury-Haddad, H.; Awwad, S. W.; Guttmann-Raviv, N.; Ayoub, N., KDM4C (GASC1) lysine demethylase is associated with mitotic chromatin and regulates chromosome segregation during mitosis. *Nucleic Acids Res.* **2014**, *42* (10), 6168-82.

(11) Luo, W.; Chang, R.; Zhong, J.; Pandey, A.; Semenza, G. L., Histone demethylase JMJD2C is a coactivator for hypoxia-inducible factor 1 that is required for breast cancer progression. *Proc. Natl. Acad. Sci. USA* **2012**, *109* (49), E3367-76.

(12) Black, J. C.; Atabakhsh, E.; Kim, J.; Biette, K. M.; Van Rechem, C.; Ladd, B.; Burrowes, P. D.; Donado, C.; Mattoo, H.; Kleinstiver, B. P.; Song, B.; Andriani, G.; Joung, J. K.; Iliopoulos, O.; Montagna, C.; Pillai, S.; Getz, G.; Whetstine, J. R., Hypoxia drives transient site-specific copy gain and drug-resistant gene expression. *Genes Dev.* **2015**, *29* (10), 1018-31.

(13) Tausendschon, M.; Dehne, N.; Brune, B., Hypoxia causes epigenetic gene regulation in macrophages by attenuating Jumonji histone demethylase activity. *Cytokine* **2011**, *53* (2), 256-62.

(14) Black, J. C.; Manning, A. L.; Van Rechem, C.; Kim, J.; Ladd, B.; Cho, J.; Pineda, C. M.; Murphy, N.; Daniels, D. L.; Montagna, C.; Lewis, P. W.; Glass, K.; Allis, C. D.; Dyson, N. J.; Getz, G.; Whetstine, J. R., KDM4A lysine demethylase induces site-specific copy gain and rereplication of regions amplified in tumors. *Cell* **2013**, *154* (3), 541-55.

(15) Liu, G.; Bollig-Fischer, A.; Kreike, B.; van de Vijver, M. J.; Abrams, J.; Ethier, S. P.; Yang, Z. Q., Genomic amplification and oncogenic properties of the GASC1 histone demethylase gene in breast cancer. *Oncogene* **2009**, *28* (50), 4491-500.

(16) Shi, L.; Sun, L.; Li, Q.; Liang, J.; Yu, W.; Yi, X.; Yang, X.; Li, Y.; Han, X.; Zhang, Y.; Xuan, C.; Yao, Z.; Shang, Y., Histone demethylase JMJD2B coordinates H3K4/H3K9 methylation and promotes hormonally responsive breast carcinogenesis. *Proc. Natl. Acad. Sci. USA* **2011**, *108* (18), 7541-6.

(17) Yamamoto, S.; Tateishi, K.; Kudo, Y.; Yamamoto, K.; Isagawa, T.; Nagae, G.; Nakatsuka, T.; Asaoka, Y.; Ijichi, H.; Hirata, Y.; Otsuka, M.; Ikenoue, T.; Aburatani, H.; Omata, M.; Koike, K., Histone demethylase KDM4C regulates sphere formation by mediating the cross talk between Wnt and Notch pathways in colonic cancer cells. *Carcinogenesis* **2013**, *34* (10), 2380-8.

(18) Yang, Z.-Q.; Imoto, I.; Fukuda, Y.; Pimkhaokham, A.; Shimada, Y.; Imamura, M.; Sugano, S.; Nakamura, Y.; Inazawa, J., Identification of a novel gene, *GASC1*, within an amplicon at 9p23–24 frequently detected in esophageal cancer cell lines. *Cancer Res.* **2000**, *60* (17), 4735.

(19) Young, L. C.; Hendzel, M. J., The oncogenic potential of Jumonji D2 (JMJD2/KDM4) histone demethylase overexpression. *Biochem. Cell Biol.* **2013**, *91* (6), 369-77.

(20) Das, P. P.; Shao, Z.; Beyaz, S.; Apostolou, E.; Pinello, L.; De Los Angeles, A.; O'Brien, K.; Atsma, J. M.; Fujiwara, Y.; Nguyen, M.; Ljuboja, D.; Guo, G.; Woo, A.; Yuan, G. C.; Onder, T.; Daley, G.; Hochedlinger, K.; Kim, J.; Orkin, S. H., Distinct and combinatorial functions of Jmjd2b/Kdm4b and Jmjd2c/Kdm4c in mouse embryonic stem cell identity. *Mol. Cell* **2014**, *53* (1), 32-48.

(21) Loh, Y. H.; Zhang, W.; Chen, X.; George, J.; Ng, H. H., Jmjd1a and Jmjd2c histone H3 Lys 9 demethylases regulate self-renewal in embryonic stem cells. *Genes Dev.* **2007**, *21* (20), 2545-57.

(22) Lohse, B.; Kristensen, J. L.; Kristensen, L. H.; Agger, K.; Helin, K.; Gajhede, M.; Clausen, R. P., Inhibitors of histone demethylases. *Bioorg. Med. Chem.* **2011**, *19* (12), 3625-36.

(23) McAllister, T. E.; England, K. S.; Hopkinson, R. J.; Brennan, P. E.; Kawamura, A.; Schofield, C. J., Recent progress in histone demethylase inhibitors. *J. Med. Chem.* **2016**, *59* (4), 1308-29.

(24) Thinnes, C. C.; England, K. S.; Kawamura, A.; Chowdhury, R.; Schofield, C. J.; Hopkinson, R. J., Targeting histone lysine demethylases—progress, challenges, and the future. *Biochim. Biophys. Acta* **2014**, *1839* (12), 1416-32.

(25) Lassalas, P.; Gay, B.; Lasfargeas, C.; James, M. J.; Tran, V.; Vijayendran, K. G.; Brunden, K. R.; Kozlowski, M. C.; Thomas, C. J.; Smith, A. B., 3rd; Huryn, D. M.; Ballatore, C., Structure property relationships of carboxylic acid isosteres. *J. Med. Chem.* **2016**, *59* (7), 3183-203.

(26) Kruidenier, L.; Chung, C. W.; Cheng, Z.; Liddle, J.; Che, K.; Joberty, G.; Bantscheff, M.; Bountra, C.; Bridges, A.; Diallo, H.; Eberhard, D.; Hutchinson, S.; Jones, E.; Katso, R.; Leveridge, M.; Mander, P. K.; Mosley, J.; Ramirez-Molina, C.; Rowland, P.; Schofield, C. J.; Sheppard, R. J.; Smith, J. E.; Swales, C.; Tanner, R.; Thomas, P.; Tumber, A.; Drewes, G.; Oppermann, U.; Patel, D. J.; Lee, K.; Wilson, D. M., A selective jumonji H3K27 demethylase inhibitor modulates the proinflammatory macrophage response. *Nature* **2012**, *488* (7411), 404-8.

(27) Taylor, F. C.; Huffman, M.; Ebrahim, S., Statin therapy for primary prevention of cardiovascular disease. *JAMA* **2013**, *310* (22), 2451-2.

(28) Maxwell, P. H.; Eckardt, K. U., HIF prolyl hydroxylase inhibitors for the treatment of renal anaemia and beyond. *Nat. Rev. Nephrol.* **2016**, *12* (3), 157-68.

(29) Rose, N. R.; Ng, S. S.; Mecinovic, J.; Lienard, B. M.; Bello, S. H.; Sun, Z.; McDonough, M. A.; Oppermann, U.; Schofield, C. J., Inhibitor scaffolds for 2-oxoglutarate-dependent histone lysine demethylases. *J. Med. Chem.* **2008**, *51* (22), 7053-6.

(30) Westaway, S. M.; Preston, A. G.; Barker, M. D.; Brown, F.; Brown, J. A.; Campbell, M.; Chung, C. W.; Diallo, H.; Douault, C.; Drewes, G.; Eagle, R.; Gordon, L.; Haslam, C.; Hayhow, T. G.; Humphreys, P. G.; Joberty, G.; Katso, R.; Kruidenier, L.; Leveridge, M.; Liddle, J.; Mosley, J.; Muelbaier, M.; Randle, R.; Rioja, I.; Rueger, A.; Seal, G. A.; Sheppard, R. J.; Singh, O.; Taylor, J.; Thomas, P.; Thomson, D.; Wilson, D. M.; Lee, K.; Prinjha, R. K., Cell penetrant inhibitors of the KDM4 and KDM5 families of histone lysine demethylases. 1. 3-Amino-4-pyridine carboxylate derivatives. *J. Med. Chem.* **2016**, *59* (4), 1357-69.

(31) Bonaldi, T.; Imhof, A.; Regula, J. T., A combination of different mass spectroscopic techniques for the analysis of dynamic changes of histone modifications. *Proteomics* **2004**, *4* (5), 1382-96.

(32) Noberini, R.; Pruneri, G.; Minucci, S.; Bonaldi, T., Mass-spectrometry analysis of histone post-translational modifications in pathology tissue using the PAT-H-MS approach. *Data Brief* **2016**, *7*, 188-94.

(33) Smith, C. M.; Haimberger, Z. W.; Johnson, C. O.; Wolf, A. J.; Gafken, P. R.; Zhang, Z.; Parthun, M. R.; Gottschling, D. E., Heritable chromatin structure: mapping "memory" in histones H3 and H4. *Proc. Natl. Acad. Sci. USA* **2002**, *99* (Suppl 4), 16454-61.

(34) Soldi, M.; Cuomo, A.; Bonaldi, T., Improved bottom-up strategy to efficiently separate hypermodified histone peptides through ultra-HPLC separation on a bench top Orbitrap instrument. *Proteomics* **2014**, *14* (19), 2212-25.

(35) Williams, S. T.; Walport, L. J.; Hopkinson, R. J.; Madden, S. K.; Chowdhury, R.; Schofield, C. J.; Kawamura, A., Studies on the catalytic domains of multiple JmjC oxygenases using peptide substrates. *Epigenetics* **2014**, *9* (12), 1596-603.

(36) Tao, Z. F.; Hasvold, L.; Wang, L.; Wang, X.; Petros, A. M.; Park, C. H.; Boghaert, E. R.; Catron, N. D.; Chen, J.; Colman, P. M.; Czabotar, P. E.; Deshayes, K.; Fairbrother, W. J.; Flygare, J. A.; Hymowitz, S. G.; Jin, S.; Judge, R. A.; Koehler, M. F.; Kovar, P. J.; Lessene, G.; Mitten, M. J.; Ndubaku, C. O.; Nimmer, P.; Purkey, H. E.; Oleksijew, A.; Phillips, D. C.; Sleebs, B. E.; Smith, B. J.; Smith, M. L.; Tahir, S. K.; Watson, K. G.; Xiao, Y.; Xue, J.; Zhang, H.; Zobel, K.; Rosenberg, S. H.; Tse, C.; Leverson, J. D.; Elmore, S. W.; Souers, A. J., Discovery of a potent and selective BCL-XL inhibitor with in vivo activity. *ACS Med. Chem. Lett.* **2014**, *5* (10), 1088-93.

(37) Durkin, K.; Fisher, L. E.; Meili, A.; Scalone, M.; Shi, X.; Vitale, J. Process for synthesis of amino-methyl tetralin derivatives US2010/0160682

For Table of Contents Use Only

Design of KDM4 Inhibitors with Anti-Proliferative Effects in Cancer Models

Young K. Chen,[†] Tiziana Bonaldi,[#] Alessandro Cuomo,[#] Joselyn R. Del Rosario,[†] David J. Hosfield,[ϕ] Toufike Kanouni,[†] Shih-chu Kao,[‡] Chon Lai,[†] Neethan A. Lobo,[‡] Jennifer Matuszkiewicz,[†] Andrew McGeehan,[‡] Shawn M. O'Connell,[†] Lihong Shi,[†] Jeffrey A. Stafford,[†] Ryan K. Stansfield,[†] James M. Veal,[†] Michael S. Weiss,[‡] Natalie Y. Yuen,[‡] and Michael B. Wallace[†*]

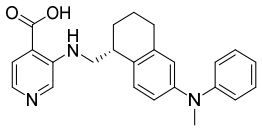

6 (QC6352)